Vibrational Structures of Dimethyl Sulfide and Ethylene Sulfide Cations Studied by Vacuum-Ultraviolet Mass-Analyzed Threshold Ionization (MATI) Spectroscopy

Sunyoung Choi, Kyo-Won Choi, and Sang Kyu Kim*

Department of Chemistry and School of Molecular Sciences (BK21), Korea Advanced Institute of Science and Technology (KAIST), Daejeon (301-750), Republic of Korea

Sangyoon Chung and Sungyul Lee

College of Environmental Science and Applied Chemistry (BK21), Kyunghee University, Kyungki-do, 449-701, Republic of Korea

Received: August 8, 2006; In Final Form: October 11, 2006

Adiabatic ionization energies of dimethyl sulfide (DMS) and ethylene sulfide (thiirane) are both accurately and precisely determined to be 8.6903 ± 0.0009 and 9.0600 ± 0.0009 eV, respectively, by vacuum-UV mass-analyzed threshold ionization (MATI) spectroscopy. Also reported are vibrational frequencies of DMS and thiirane monocations. Simulations using a Franck−Condon analysis based on ab initio molecular structures reproduce the experimental findings quite well. Detailed vibrational structures are discussed with the aid of ab initio calculations. Ionization-induced structural changes provide the information about the role of the sulfur nonbonding orbital in the geometrical layout of the title compounds.

I. Introduction

Sulfur is abundant in nature, and its thermochemical cycle is very important for understanding the properties and controlling the chemical reactions of sulfur-containing compounds. One essential property is the ionization potential (IP). Variation of the IP according to chemical substitution is an interesting aspect of sulfur chemistry, especially because the highest-occupied molecular orbital (HOMO) is usually the nonbonding orbital localized on sulfur. Delocalization of this orbital over the entire molecule in various chemical environments could be reflected in the difference of the IP value. In this work, we have studied ionization spectroscopy of two of the simplest sulfides, dimethyl sulfide (DMS) and ethylene sulfide (thiirane). Although there have been a number of spectroscopic studies on the ionization behavior of these molecules,[1−22] we provide here the most accurate and precise ionization potential to date along with the measurements of vibrational frequencies of the cation ground state.

DMS is the major natural source of sulfur to the atmosphere, and it plays a pivotal role in regulating the sulfur cycle and the amount of radiation the Earth reflects.[23] Thus, radiation-induced ionization and associated thermochemical cycles in the atmosphere have been studied intensively for many decades. Accordingly, there have been a number of reports of the ionization potential of DMS.[1−13] These include UV or vacuum ultraviolet (VUV) Rydberg,[1−5] photoelectron,[6−9] photoionization,[10] and electron impact spectroscopy.[11−12] The ionization spectroscopy of thiirane, in which two carbons adjacent to sulfur are covalently bonded to form a cyclic structure, has also been studied intensively.[14−22] For thiirane, because of its cyclic structure, the ring strain energy[8] and photochemical cleavage leading to ring-opening[11,21−22,24] have been intriguing issues for many years. In spite of numerous studies on the ionization behavior of DMS and thiirane, more reliable and accurate spectroscopic values are still needed. Nowadays, the most precise measurement of IP can be achieved by use of the zero electron kinetic energy (ZEKE) or mass-analyzed threshold ionization (MATI) spectroscopy.[25] For the last two decades, ZEKE and/or MATI of a variety of molecules have been carried out to give valuable information about chemical properties such as DNA base ionization,[26,27] conformer-specific ionization[28] and cluster chemistry.[29,30] Vacuum-UV MATI spectroscopy is particularly useful for molecules of which the intermediate state is hardly accessible, for example, due to its ultrashort lifetime. Here, we apply the VUV-MATI technique to identify important spectroscopic features of DMS and thiirane in the ionization threshold region. The ionization potential and cationic vibrational structure of the title molecules are determined and interpreted with the aid of ab initio calculations and Franck−Condon analysis.

II. Experimental Section

DMS and thiirane were purchased from Aldrich and used without further purification. The compounds were mixed with Ar carrier gas and expanded into the vacuum chamber through a nozzle orifice (General valve, 0.5 mm diameter orifice) with a backing pressure of ∼2 atm and a repetition rate of 10 Hz. The molecular beam chamber was pumped with two molecular turbo pumps to maintain the background pressure of 10^{-7} Torr when the nozzle was on. The molecular beam was directed through a 1-mm-diameter skimmer (Precision Instrument Services) before it was overlapped with the laser pulse. The third harmonic output of Nd:YAG laser (Continuum, Precision 2) was split in half to pump two independent dye lasers. One (Lambdaphysik, Scanmate 2) generated the laser pulse that was frequency-doubled through a BBO crystal to give the UV laser pulse at 212.552 nm. The other dye laser (Lumonics, HD-500) was used to generate the tunable visible laser pulse in the 414−

* Corresponding author. Fax: +82-42-869-2810. E-mail: sangkyukim@kaist.ac.kr.

10.1021/jp0651079 CCC: $33.50
Published on Web 11/18/2006

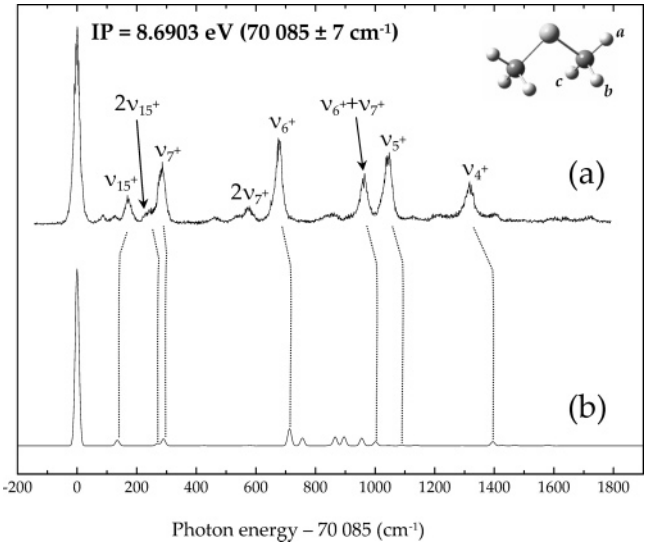

Figure 1. (a) VUV-MATI spectrum of DMS. (b) The simulation calculated by the Franck−Condon analysis based on ab initio molecular geometries (see Table 3).

560 nm range. The UV laser was used to excite the Kr $5p[1/2]_0 - 4p^6$ transition while the visible laser was used to tune the vacuum-UV (VUV) laser output via the four-wave mixing process. The generated VUV radiation was separated from UV and visible fundamentals by using the edge of the CaF_2 collimating lens on the exit of the Kr cell. The VUV laser excited the molecule to high-*n* Rydberg states to be pulsed-field ionized after the delay time of 10−15 μs. The generated ions were accelerated, drifted along the time-of-flight axis, and detected by dual microchannel plates. Ion signals were digitized by an oscilloscope (LeCroy, LT584M) and stored in a personal computer. The long delay time between the laser excitation and pulsed field ionization made it possible to separate out the MATI signal from the directly formed ion signal without the use of a spoil field. The electric field used for the pulsed field ionization was maintained below 10 V/cm to obtain highly resolved MATI spectra.

Computational Details. All calculations were carried out using the Gaussian03 electronic structure package.[31] The minimum energy geometries and normal modes of DMS and thiirane in the ground neutral and cation states were calculated by the B3LYP density functional theory (DFT)[32,33] and the Moller−Plesset second-order (MP2) perturbation theory[34] using the 6-311++G(d,p) basis set. We have calculated Franck−Condon overlap integrals by using the Duschinsky transformation[35] using the code developed by Peluso and cowokers.[36,37]

III. Results and Discussion

A. Structure of DMS^+ (D_0). DMS and thiirane are of C_{2v} symmetry. The ground state of DMS has the electron configuration $(2b_1)^2(7a_1)^2(4b_2)^2(1a_2)^2(5b_2)^2(8a_1)^2(3b_1)^2$. The highest-occupied molecular orbital (HOMO) with $3b_1$ symmetry is oriented perpendicular to the molecular plane.[5] Because the HOMO has 3p character localized on the sulfur atom, the removal of an electron from HOMO is not expected to induce a drastic structural change. Accordingly, the VUV-MATI spectrum of DMS in Figure 1 shows the strong origin peak located at 70 085 cm^{-1}. This peak position is measured as a function of the pulsed-field strength, plotted versus the square root of the electric field in V/cm, and extrapolated to give the adiabatic ionization energy of 8.6903 ± 0.0009 eV. This value is close to previously reported ionization potentials within errors as listed in Table 1. It is noteworthy that there has been great effort to obtain an accurate IP measurement because of the

TABLE 2: Vibrational Frequencies of DMS (S_0) and DMS^+(D_0), cm^{-1}

		neutral[a]		cation (D_0)			description
		IR	Raman	B3LYP	MP2	expt	
a_1	ν_1	2980		3160	3222		C−H stretch
	ν_2	2935	2910	3019	3075		C−H stretch
	ν_3	1434		1442	1464		CH_3 deformation
	ν_4	1327	1331	1350	1395	1315	CH_3 deformation
	ν_5	1022	1032	1069	1089	1044	CH_3 rock
	ν_6	684	691	658	713	678	C−S stretch
	ν_7		284	278	290	284	C−S−C deformation
a_2	ν_8		2982	3090	3173		C−H stretch
	ν_9		1428	1408	1436		
	ν_{10}			879	896		
	ν_{11}			7	−46		CH_3 torsion
b_1	ν_{12}			3091	3174		C−H stretch
	ν_{13}			1434	1456		
	ν_{14}			839	866		
	ν_{15}			113	135	172	CH_3 torsion
b_2	ν_{16}			3158	3221		C−H stretch
	ν_{17}			3010	3072		C−H stretch
	ν_{18}			1412	1436		
	ν_{19}			1328	1369		CH_3 deformation
	ν_{20}			930	955		CH_3 rock
	ν_{21}			695	756		C−S stretch

[a] Reference 38.

TABLE 3: Minimum Energy Structures of the Neutral and Cationic Ground States of DMS Calculated at the MP2 Level with the Basis Set of 6-311++G(d,p)

	neutral		
	calcd	obsd[a]	cation (D_0)
R(S−C)	1.803	1.802 ± 0.002	1.784
R(C−H_a)	1.092	1.091	1.090
R(C−H_b)	1.093	1.091 ± 0.005	1.094
∠H_aCS	107.66	106.38	108.07
∠H_aCH_b	108.49	109.36 ± 0.20	110.75
∠H_bCH_c	109.70	109.32 ± 0.20	109.75
∠CSC	98.09	98.52 ± 0.10	102.13
∠H_aCSC	180.00		180.00

[a] Reference 39.

TABLE 1: Ionization Potentials of DMS and Thiirane (eV)

DMS	thiirane	method	ref (year)
8.6903 ± 0.0009	9.0600 ± 0.0009	VUV-MATI	this work
8.73	9.08	calcd	11 (1961)
8.685 ± 0.005	9.051 ± 0.003	PI	10 (1962), 22 (2005)
	9.04 ± 0.041	PI	21 (1982)
8.7	8.870 ± 0.15	EI	12 (1963), 11 (1961)
8.710 ± 0.005	9.06 ± 0.01	PES	9 (1995), 19 (1994)
8.54	8.93	PES	8 (1980)
8.65	9.05	PES	7 (1972), 18 (1973)
8.68 ± 0.03		PES	6 (1969)
8.68	9.072 ± 0.008	VUV absorption	4 (1974), 16 (1989)
8.706 ± 0.010		VUV absorption	3 (1973)

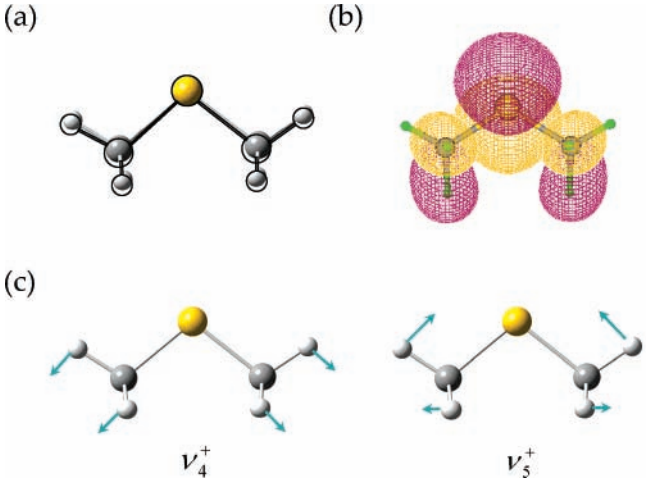

Figure 2. (a) Ab initio (MP2) calculated minimum energy structures of DMS in the neutral (circle and rod) and cationic (ball and stick) ground states. (b) Singly occupied molecular orbital (SOMO) of DMS cation. (c) Normal-mode descriptions for ν_4^+(CH_3 deformation) and ν_5^+ (CH_3 rock) modes.

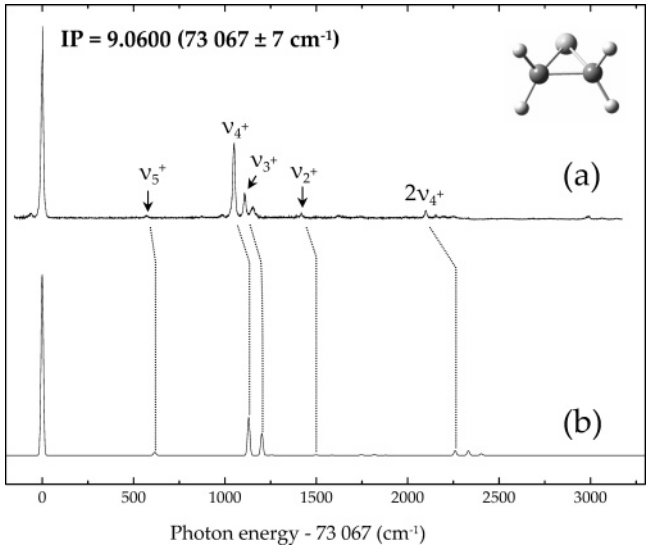

Figure 3. (a) VUV-MATI spectrum of thiirane. (b) The simulated spectrum calculated by the Franck−Condon analysis using ab initio molecular structures at the MP2 level (see Table 5).

importance of atmospheric sulfur chemistry. In this sense, the IP value in this work is quite meaningful because it provides the most precise and accurate IP of DMS to date, which should be utilized for the refinement of associated thermochemical properties. The VUV-MATI spectrum provides the vibrational frequencies of the DMS cation. While vibrational frequency values provide associated force constants, relative band intensities reflect the respective DMS structural change upon ionization. The MATI spectrum of DMS in Figure 1 is quite simple and peak assignments are straightforward. Because the ionization process leaves the nuclear momenta frozen, the vibrational wavefunction overlap integral determines the peak intensity of each band. Naturally, only the totally symmetric vibrational bands are found be significantly observed. Vibrational frequencies of DMS^+ are in good agreement with those calculated (Table 2). The whole spectrum can be reproduced with the aid of the Franck−Condon analysis based on neutral and cation structures calculated at the MP2 level (Table 3). The calculation predicts C−S bond shortening and the increase of the C−S−C angle. This structural change indicates that vibrational modes corresponding to C−S stretching (ν_6^+) and C−S−C bending

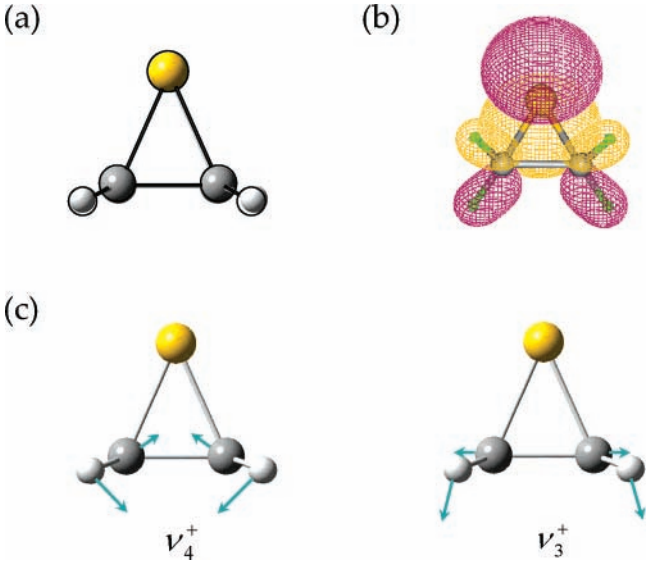

Figure 4. (a) Ab initio (MP2) calculated minimum energy structures of thiirane in the neutral (circle and rod) and cationic (ball and stick) ground states. (b) Singly occupied molecular orbital (SOMO) of thiirane cation. (c) Normal-mode descriptions for ν_4^+ (CH_2 wag + ring breath) and ν_5^+ (CH_2 wag + C−C stretch) modes.

(ν_7^+) should be Franck−Condon active supported by a simulation based on the Franck−Condon analysis and ab initio calculations in Figure 1. Strong overtones and combination bands of ν_6^+ and ν_7^+ are also observed. The simulation is in accord with experiment, showing that ab initio molecular structures of neutral and cationic ground states are quite reliable for DMS though fine adjustments in theory are still necessary. For instance, the CH_3 rock mode (ν_5^+) of which normal-mode description is given in Figure 2, is quite strongly observed in the experiment, although it is predicted by the simulation to be much less excited. Meanwhile, the CH_3 deformation mode (ν_4^+) in Figure 2 is only weakly observed whereas the Franck−Condon overlap integral is predicted to be large, suggesting that the movement of the methyl moiety upon ionization is relatively poorly predicted by theory. The ionization-induced structural change reflects the role of the nonbonding HOMO in the structural nuclear framework of DMS. From the point of the simple valence-shell electron pair repulsion (VSEPR) theory, the repulsion between the nonbonding pair and two C−S bonding pairs would decrease when one electron in the nonbonding pair is removed. This simple interpretation is sufficient to explain the qualitative trend of the structural change upon ionization. The calculated orbital diagram is indeed showing this trend correctly. The single-occupied molecular orbital (SOMO) of the DMS cation in Figure 2 shows the antibonding character along two C−S bonds. The electron deficiency in this orbital of the DMS cation, therefore, induces the shortening of the C−S bond distance.

B. Structure of Thiirane$^+$ (D_0). The molecular framework of thiirane is more rigid compared with that of DMS. The electronic configuration of thiirane in the ground state is $(2b_1)^2(7a_1)^2(1a_2)^2(8a_1)^2(4b_2)^2(3b_1)^2$. The HOMO of thiirane is also of 3p-like character localized on sulfur.[14] The adiabatic ionization energy of thiirane is determined to be 9.0600 ± 0.0009 eV. This value is consistent with earlier reported IP values in Table 1. The ionization energy of thiirane is ~0.37 eV higher than that of DMS. The higher ionization energy of thiirane had been ascribed to the d-orbital participation in the C−S bonding of ethylene sulfide leading to the stabilization of the HOMO.[18]

TABLE 4: Vibrational Frequencies of Thiirane in the Neutral and Cationic Ground States (cm^{-1})

		neutral[a]		cation (D_0)			
		IR	Raman	B3LYP	MP2	expt	description
a_1	ν_1	3013.5		3108	3162		C−H stretch
	ν_2	1456.8	1450	1474	1499	1417	CH_2 scissor
	ν_3	1109.9	1112	1174	1202	1108	CH_2 wag + C−C stretch
	ν_4	1024	1025	1088	1130	1048	CH_2 wag. + ring breath
	ν_5	627.3	611.3	559	616	571	C−S stretch
a_2	ν_6			3187	3255		C−H stretch
	ν_7			1201	1224		
	ν_8		895	846	875		CH_2 twist
b_1	ν_9	3088.0	3071.7	3206	3272		C−H stretch
	ν_{10}	945.2	944	897	941		CH_2 twist
	ν_{11}	824.3	822	777	792		CH_2 rock
b_2	ν_{12}	3013.0		3098	3155		C−H stretch
	ν_{13}	1435.9	1431	1441	1467		CH_2 scissor
	ν_{14}	1050.8		1114	1157		CH_2 wag
	ν_{15}		650.8	542	628		C−S stretch

[a] Reference 40.

TABLE 5: Minimum Energy Structures of the Neutral and Cationic Ground States of Thiirane Calculated at the MP2 Level with a 6-311++G(d,p) Basis Set

	neutral		
	calcd	obsd[a]	cation (D_0)
R(S−C)	1.814	1.815	1.828
R(C−C)	1.487	1.484	1.473
R(C−H)	1.085	1.083	1.088
∠CSC	48.39	48.16	47.52
∠HCH	115.62	115.50	116.33
∠HCC	117.77		119.45
∠HCS	115.25		111.89

[a] Reference 41.

Aue et al.[12] reported a detailed study of the ionization of three-membered-ring heterocycle compounds. According to them, the delocalization of the $3b_1$ orbital that gets severe as the C−S−C angle decreases is responsible for the increased IP of thiirane compared to that of DMS. However, the origin of the higher IP of thiirane compared to other sulfides seems to be still in controversy especially in terms of whether or not the ring strain energy is responsible for this.

The MATI spectrum of thiirane is even simpler than that of DMS (Figure 3). The most intensive vibronic peak is located at 1048 cm^{-1}, which corresponds to the ring-breathing mode (ν_4^+). The band at 1108 cm^{-1} is also strongly observed and assigned to the C−C stretching mode (ν_3^+). These normal modes are depicted in Figure 4. Ab initio calculations have been carried out for comparison with experiment. All other weakly observed bands were assigned with the aid of the Franck−Condon analysis based on ab initio molecular structures of thiirane in S_0 and D_0. In Table 4, ab initio vibrational frequencies of thiirane$^+$ are listed to be compared with the experiment. Also listed are vibrational frequencies of neutral thiirane in the ground state. The spectral simulation shown in Figure 3b matches the experiment very nicely, indicating that the MP2 calculation predicts the cationic geometry quite well. The ionization induces the increase of the C−S bond length, whereas it causes the decrease of the C−C bond distance and C−S−C angle, Figure 4 and Table 5. The SOMO is mainly localized on sulfur (Figure 4) and it seems to not be straightforward to infer the ionization-driven structural change just from the inspection of the SOMO in this case in which the ring strain energy is quite high. This structural change is also consistent with strong ν_3^+ and ν_4^+ excitation, obvious by the inspection of the corresponding normal-mode descriptions in Figure 4. The fact that the C−S−C angle decreases upon ionization may suggest that the ring strain energy becomes larger in the thiirane cation. The larger ring strain energy in the cation compared to the ring strain energy in the neutral ground state is intuitively consistent with the higher IP of thiirane compared to the IP of DMS. A photodissociation dynamic study of both the neutral and cationic state of thiirane would be quite useful for unraveling the effect of ring strain energy on energetics in general. The determination of an accurate IP and vibrational structure of the cation will aid in unraveling the energetics involved in the formation of cyclic ring compounds.

IV. Summary and Conclusions

In this work, the adiabatic ionization energies of dimethyl sulfide and ethylene sulfide are accurately and precisely determined to be 8.6903 ± 0.0009 and 9.0600 ± 0.0009 eV, respectively. VUV-MATI spectroscopy also provides the cationic vibrational structures of both molecules. The spectral simulation using the Franck−Condon analysis based on ab initio calculations is quite successful in the interpretation of experimental findings. Ionization-induced structural changes of DMS and thiirane are well supported by MP2 calculations. However, further theoretical improvement is necessary, especially in the case of DMS. VUV-MATI spectroscopic results and their interpretation based on ab initio calculations and Franck−Condon analysis are extremely useful in studying ionization-induced structural changes of various chemical systems. Because the neutral excited state is not well understood in many cases, the direct ionization by VUV seems to have the great advantage for this purpose.

Acknowledgment. The work was financially supported by Korea Science and Engineering Foundation (No. R01-2005-000-10117-0).

References and Notes

(1) Clark, L. B.; Simpson, W. T. *J. Chem. Phys.* **1965**, *43*, 3666.
(2) Thompson, S. D.; Carroll, D. G.; O'Donnell, M.; McGlynn, S. P. *J. Chem. Phys.* **1966**, *45*, 1367.
(3) Scott, J. D.; Causley, G. C.; Russell, B. R. *J. Chem. Phys.* **1973**, *59*, 6577.
(4) McDiarmid, R. *J. Chem. Phys.* **1974**, *61*, 274.
(5) Tokue, I. *J. Chem. Phys.* **1989**, *91*, 2808.
(6) Altenloh, D. D.; Russell, B. R. *Chem. Phys. Lett.* **1981**, *77*, 217.
(7) Gallegos, E.; Kiser, R. W. *J. Phys. Chem.* **1961**, *65*, 1177.
(8) Hobrock, B. G.; Kiser, R. W. *J. Phys. Chem.* **1963**, *67*, 1283.
(9) Watanabe, K.; Nakayama, T.; Mottl, J. *J. Quant. Spectrosc. Radiat. Transfer* **1962**, *2*, 369

(10) Cullen, W. D.; Frost, D. C.; Vroom, D. A. *Inorg. Chem.* **1969**, *8*, 1803.
(11) Frost, D. C.; Herring, F. G.; Katrib, A.; McDowell, C. A.; McLean, R. A. N. *J. Phys. Chem.* **1972**, *76*, 1030.
(12) Aue, D. H.; Webb, H. M.; Davidson, W. R.; Vidal, M.; Bowers, M. T.; Goldwhite, H; Vertal, L. E.; Douglas, J. E.; Kollman, P. A.; Kenyon, G. L. *J. Am. Chem. Soc.* **1980**, *102*, 5151.
(13) Morgan, R. A.; et al. *J. Chem. Soc., Faraday Trans.* **1995**, *91*, 3339.
(14) Clark, L. B.; Simpson, W. T. *J. Chem. Phys.* **1965**, *43*, 3666.
(15) Basco, N.; Morse, R. D. *Chem. Phys. Lett.* **1973**, *20*, 404.
(16) Tokue, I. *J. Chem. Phys.* **1989**, *91*, 2808.
(17) Carnell, M.; Peyerimhoff, S. D. *Chem. Phys. Lett.* **1993**, *212*, 654.
(18) Frost, D. C.; Herring, F. G.; Kartrib, A.; McDwell, C. A. *Chem. Phys. Lett.* **1973**, *20*, 401.
(19) Morgan, R. A.; Puyuelo, P.; Howe, J. D.; Ashfold, M. N. R.; Buma, W. J.; Milan, J. B.; de Lange, C. A. *J. Chem. Soc., Faraday Trans.* **1994**, *90*, 3591.
(20) Schweig, A.; Thiel, W. *Chem. Phys. Lett.* **1973**, *21*, 541.
(21) Butler, J. J.; Baer, T. *J. Am. Chem. Soc.* **1982**, *104*, 5016.
(22) Chiang, S.-Y.; Fang, Y.-S. *J. Electron Spectrosc. Relat. Phenom.* **2005**, *144*, 223.
(23) Arsene, T. W.; Andreae, M. O.; Schebeske, G. *J. Geophys. Res.* **1994**, *99*, 22819.
(24) Qi, F.; Sorkhabi, O.; Suits, A. G.; Chien, S.-H.; Li, W.-K. *J. Am. Chem. Soc.* **2001**, *123*, 148.
(25) Müllor-Dethlefs, K.; Schlag, E. W. *Annu. Rev. Phys. Chem.* **1991**, *42*, 109.
(26) Choi, K.-W.; Lee, J.-H.; Kim, S. K. *J. Am. Chem. Soc.* **2005**, *127*, 15674.
(27) Choi, K.-W.; Lee, J.-H.; Kim, S. K. *Chem. Commun.* **2006**, *1*, 78.
(28) Park, S. T.; Kim, S. K.; Kim, M. S. *Nature* **2002**, *415*, 306.
(29) Baek, S. J.; Choi, K.-W.; Choi, Y. S.; Kim, S. K. *J. Phys. Chem. A.* **2003**, *107*, 4826.
(30) Choi, K.-W.; Ahn, D.-S.; Lee, S.; Kim, S. K. *J. Phys. Chem. A.* **2004**, *108*, 11292.
(31) Frisch, M. J.; Trucks, G. W.; Schlegel, H. B.; Scuseria, G. E.; Robb, M. A.; Cheeseman, J. R.; Montgomery, J. A., Jr.; Vreven, T.; Kudin, K. N.; Burant, J. C.; Millam, J. M.; Iyengar, S. S.; Tomasi, J.; Barone, V.; Mennucci, B.; Cossi, M.; Scalmani, G.; Rega, N.; Petersson, G. A.; Nakatsuji, H.; Hada, M.; Ehara, M.; Toyota, K.; Fukuda, R.; Hasegawa, J.; Ishida, M.; Nakajima, T.; Honda, Y.; Kitao, O.; Nakai, H.; Klene, M.; Li, X.; Knox, J. E.; Hratchian, H. P.; Cross, J. B.; Bakken, V.; Adamo, C.; Jaramillo, J.; Gomperts, R.; Stratmann, R. E.; Yazyev, O.; Austin, A. J.; Cammi, R.; Pomelli, C.; Ochterski, J. W.; Ayala, P. Y.; Morokuma, K.; Voth, G. A.; Salvador, P.; Dannenberg, J. J.; Zakrzewski, V. G.; Dapprich, S.; Daniels, A. D.; Strain, M. C.; Farkas, O.; Malick, D. K.; Rabuck, A. D.; Raghavachari, K.; Foresman, J. B.; Ortiz, J. V.; Cui, Q.; Baboul, A. G.; Clifford, S.; Cioslowski, J.; Stefanov, B. B.; Liu, G.; Liashenko, A.; Piskorz, P.; Komaromi, I.; Martin, R. L.; Fox, D. J.; Keith, T.; Al-Laham, M. A.; Peng, C. Y.; Nanayakkara, A.; Challacombe, M.; Gill, P. M. W.; Johnson, B.; Chen, W.; Wong, M. W.; Gonzalez, C.; Pople, J. A. *Gaussian 03*, revision C.02; Gaussian, Inc.: Wallingford, CT, 2004.
(32) Becke, A. D. *J. Chem. Phys.* **1993**, *98*, 5648.
(33) Lee, C.; Yang, W.; Parr, R. G. *Phys. Rev. B* **1988**, *37*, 785.
(34) Möller, C.; Plesset, M. S. *Phys. Rev.* **1934**, *46*, 618.
(35) Duschinsky, F. *Acta Physicochim. URSS* **1937**, *7*, 551.
(36) Peluso, A.; Santoro, F.; Re, G. D. *Int. J. Quantum Chem.* **1997**, *63*, 233.
(37) Borrelli, R.; Peluso, A. *J. Chem. Phys.* **2003**, *119*, 8437.
(38) Allkins, J. R.; Hendra, P. J. *Spectrochim. Acta* **1966**, *22*, 2075.
(39) Pierce, L.; Hayashi, M. *J. Chem. Phys.* **1961**, *35*, 479
(40) Allen, W. D.; Bertie, J. E.; Falk, M. V.; Hess, B. A., Jr.; Mast, G. B.; Othen, D. A.; Schaad, L. J.; Schaefer, H. F., III. *J. Chem. Phys.* **1986**, *84*, 4211.
(41) Okiye, K.; Hirose, C.; Lister, D. G.; Sheridan, J. *Chem. Phys. Lett.* **1974**, *24*, 111.